Investigation of High Ozone Events due to Wildfire Smoke in an Urban Area

Crystal D. McClure[a,1] and Daniel A. Jaffe[a,b]

[a] *Department of Atmospheric Science, University of Washington, 408 ATG Building, Box 351640, Seattle, Washington, 98195, U.S.A*

[b] *School of Science, Technology, Engineering and Mathematics, University of Washington Bothell, 18115 Campus Way NE, Bothell, Washington, 98011, U.S.A.*

[1] Corresponding author. Tel: 1-425-352-3478
E-mail address: cdm0711@uw.edu

Abstract

Using data from the St. Luke's site in Meridian, ID (near Boise) during 2006-2017 and a 2017 summer intensive campaign, we investigate enhancements in ozone (O_3) during wildfire events in an urban area. We calculate a wildfire criterion based on the National Oceanic and Atmospheric Administration (NOAA) National Environmental Satellite, Data, and Information Service (NESDIS) Hazard Mapping System (HMS) smoke product and historically averaged $PM_{2.5}$ data to determine when wildfire emissions are influencing the area (smoke vs. non-smoke events). We also use a Generalized Additive Model (GAM) to investigate anomalous sources of O_3, such as wildfires, in this urban area. During the summer 2017 intensive campaign, we find that peroxyacetyl nitrate (PAN), reactive nitrogen (NO_y), and maximum daily 8 hour average (MDA8) O_3 show significant enhancements during smoke events compared with non-smoke periods (56%, 41%, and 29%, respectively). We calculate the 95% confidence interval of $\Delta PM_{2.5}/\Delta CO$, $\Delta NO_y/\Delta CO$, $\Delta PAN/\Delta NO_y$, and $\Delta PAN/\Delta CO$ enhancement ratios (ERs) to be 0.129 – 0.144 µg/m^3/ppbv, 0.018 – 0.022 ppbv/ppbv, 0.152 – 0.192 ppbv/ppbv, and 3.04 – 3.76 ppbv/ppmv, respectively, for wildfire-influenced events. We also observe an enhancement in O_3 production up to $PM_{2.5}$ concentrations of 60-70 µg/m^3 in smoke, after which we see a reduction in average MDA8 O_3 mixing ratios. We use the four highest O_3 events during summer 2017 as case studies to examine the highly variable conditions due to the influence of wildfire smoke in an urban area. In two cases, we investigate smoke days that show significant O_3 enhancement and moderate $PM_{2.5}$ concentrations. These cases suggest that ERs, such as $\Delta PM_{2.5}/\Delta CO$ and $\Delta NO_y/\Delta CO$, are less useful in determining the influence of wildfire smoke in an urban area on moderate smoke days. Another case shows reduced O_3 production during a very high, 3-day smoke event ($PM_{2.5} > 70$ µg/m^3). After this high smoke period, a 20 ppbv enhancement in

MDA8 O_3 is observed in moderate smoke. These results indicate that wildfire-influenced O_3 enhancements are highly variable in urban areas but generally increase up to around 60 μg/m^3 of $PM_{2.5}$, after which they decrease at very high smoke concentrations. This study also suggests that multiple tracer measurements are needed to fully characterize wildfire plumes in urban areas.

Keywords: Wildfires, Biomass Burning, PAN, Generalized Additive Model, Ozone, Enhancement Ratios

1. Introduction

Wildfires are a major source of pollution during the summer season in the western U.S. (Baylon et al., 2015, 2016; Briggs et al., 2016; Hallar et al., 2017; Jaffe et al., 2008a, 2008b; Laing et al., 2016; Lu et al., 2016; McClure and Jaffe, 2018; Singh et al., 2012; Spracklen et al., 2007; Urbanski et al., 2011; Wigder et al., 2013). Wildfires emit primary pollutants (e.g., particulate matter (PM), carbon monoxide (CO), nitrogen oxides (NO_x [= NO + NO_2]), and volatile organic compounds (VOCs)) and contribute to the formation of secondary pollutants (e.g., ozone (O_3) and peroxyacetyl nitrate (PAN)) (Alvarado et al., 2010; Briggs et al., 2016; Jaffe and Wigder, 2012; Lu et al., 2016; Val Martin et al., 2006). It is largely agreed that in the last few decades, large wildfires in the western U.S. have been increasing in frequency and duration due to climatological factors and human ignition (Aldersley et al., 2011; Balch et al., 2017; Dennison et al., 2014; Kitzberger et al., 2007; Littell et al., 2009; Miller and Safford, 2012; Westerling, 2016; Westerling et al., 2006). Recently, it was concluded that as a result of increasing wildfires, the 98th quantile of $PM_{2.5}$ is also increasing in the northwest U.S. (McClure and Jaffe, 2018). Modelling studies also suggest an increased probability of wildfires through the end of the century (Moritz et al., 2012; Pechony and Shindell, 2010; Spracklen et al., 2009; Val Martin et al., 2015). With the projected increase in wildfires, it is vitally important to understand how these emissions affect air quality in urban environments.

Although pollutants like PM can be emitted directly from wildfires, O_3 is formed as a secondary pollutant through the reaction of NO_x and VOCs in the presence of sunlight. Jaffe et al. (2008a, 2008b) and Lu et al. (2016) show enhancements of O_3 and PM during summer in high wildfire years. However, these enhancements are highly episodic and vary with plume age and other factors (Alvarado et al., 2010; Jaffe and Wigder, 2012). While most O_3 mixing ratios are enhanced downwind of a wildfire, some show no enhancement or a depletion in O_3 (Akagi et al., 2013, 2011; Alvarado et al., 2010; Baylon et al., 2015; Honrath et al., 2004; Jaffe and Wigder, 2012; Pfister et al., 2006; Val Martin et al., 2006; Verma et al., 2009). This discrepancy in O_3 production is likely due to NO_x-limiting conditions or possibly aerosol effects enhancing or reducing photochemical production (Alvarado et al., 2015; Baylon et al., 2018; Castro et al., 2001; Jiang et al., 2012; Palancar et al., 2013). Within the first few hours after emission, approximately 40% of NO_x within a wildfire plume can be rapidly converted to PAN as observed by Alvarado et al. (2010). PAN is a reservoir species for NO_x, meaning, NO_x can be stored as PAN, transported downwind, and then re-emitted as NO_x (Fischer et al., 2010). This mechanism could contribute to the variability of O_3 mixing ratios seen downwind of wildfires. The primary loss process for PAN is thermal decomposition. This suggests that if wildfire smoke is injected higher into the atmosphere, most NO_x could be unavailable for O_3 production during transport at low temperatures while being stored as PAN. However, when this plume descends into a warmer region, NO_x could be released by the decomposition of PAN for a significant enhancement in O_3 downwind.

Due to its effects as an irritant and health hazard, O_3 is regulated by the Clean Air Act, which requires the U.S. Environmental Protection Agency (EPA) to set National Ambient Air Quality Standards (NAAQS) for the protection of the general public. The primary standard for O_3 requires that the three-year running average of the fourth-highest maximum daily 8-hour average (MDA8) of O_3 be at or below 0.070 ppmv. Kaulfus et al. (2017) found that 20% of O_3 exceedances days (MDA8 > 0.070 ppm) occur when smoke is overhead within the continental U.S. This suggests that wildfires can be a significant contributor to NAAQS compliance for a region. Camalier et al. (2007) and Gong et al. (2017) also show that Generalized Additive

Models (GAMs) can be used to determine unusual sources of O_3 production. These statistical models use meteorological and transport variables to determine the variability of O_3. They found that when the modelled O_3 values significantly diverged from the observed data (> 95^{th} or 97.5^{th} percentile), sources of anomalous pollution (either anthropogenic or wildfire) were affecting O_3 production.

In urban areas, wildfire emissions can enhance the production of O_3 through the addition of NO_x and VOCs (Akagi et al., 2013; Singh et al., 2012). However, in a NO_x-rich environment, such as an urban area, O_3 production can decrease at very high NO_x mixing ratios (NO_x-titration). In addition, high PM concentrations from wildfire plumes can positively or negatively affect the production of O_3 (Baylon et al., 2018; Real et al., 2007; Reid et al., 2005). These factors lead to an uncertainty in the effects of wildfire-influenced O_3 production in urban areas. We aim to decipher the role of wildfire emission on O_3 production in an urban area routinely affected by wildfire smoke (Boise, Idaho) to assist in bridging this gap in knowledge.

The main goal of this analysis is to investigate the role of wildfire emissions on O_3 production in an urban area. In order to achieve this goal, we focus on these scientific questions: (1) What are the characteristic $\Delta PM_{2.5}/\Delta CO$, $\Delta NO_y/\Delta CO$, $\Delta PAN/\Delta NO_y$, and $\Delta PAN/\Delta CO$ enhancement ratios (ERs) in urban areas under the influence of wildfire emissions? (2) How do O_3 mixing ratios change with an increase in wildfire PM (smoke)? (3) How can PAN mixing ratios and/or statistical modeling be used to investigate wildfire-influenced O_3 enhancements in urban areas? To accomplish these goals, we collected PAN measurements at an established urban monitoring site that was strongly affected by wildfire smoke during summer 2017 (see Section 2.1 for the site description). We developed a wildfire criterion (described in Section 2.4) to identify when the urban area was being affected by wildfire emissions and calculated ERs for "smoke" and "no-smoke" days. We also looked at the effects of $PM_{2.5}$ on O_3 mixing ratios over 10+ years of data at the same site. Additionally, we used PAN measurements made during 2017 and the GAM results for 2007-2017 to improve our understanding of wildfire smoke effects on O_3 in urban areas. 2017 was an exceptionally high wildfire year with the second highest number of acres burned between 1983 and 2017 (NIFC, 2018).

2. Methods

2.1 St. Luke's Site

The St. Luke's National Core (NCore) urban monitoring site (43.601 °N, 166.348 °W, 824 m above sea level (asl), AQS code: 160010010) is located in Meridian, Idaho, and is maintained by the Idaho Department of Environmental Quality (IDEQ). This site is located directly east of the St. Luke's Medical Center in Meridian in an empty field and is approximately 10 km WSW of the Boise city center. Atmospheric measurements have been collected at this site since 2006. This area is strongly affected by wildfire smoke and was shown to be within the highest region of increasing fine particulate matter (diameter < 2.5 µm [$PM_{2.5}$]) due to wildfires by McClure and Jaffe (2018).

The most recent measurements taken at this site include (but are not limited to): CO [Teledyne API T300U], O_3 [Teledyne API T400], sulfur dioxide (SO_2) [Teledyne API T100U], nitrogen oxide (NO) and total reactive nitrogen oxides (NO_y [= NO + NO_2 + NO_3 + N_2O_5 + HNO_3 + HONO + PAN + …]) [Teledyne T200U], and $PM_{2.5}$ [Met One BAM-1020]. Hourly data for these pollutants were provided by the IDEQ for summer 2017. Hourly and daily data from the St. Luke's site for 2006-2017 were retrieved from the EPA Data Mart (https://www.epa.gov/outdoor-air-quality-data). In 2017, we also measured PAN at this site from

August 1st through September 30th. During this period, 28 of 61 days had wildfire smoke influence (as described by the daily smoke criterion in Section 2.4). All dates and times listed in this text are in local standard time (Mountain Standard Time (MST), UTC-7). Further details regarding measurement specifications and calibration data can be found in the supplementary information (SI).

2.2 PAN Measurement Description

PAN was measured using a custom-built gas chromatograph (GC) and Shimadzu Mini-2 Electron Capture Detector (ECD). Measurements of PAN are made at five-minute time intervals and averaged over an hour to compare with the hourly St. Luke's data provided during summer 2017. Detailed descriptions of instrument configuration and testing can be found in Fischer et al. (2010), Flocke et al. (2005), and the SI Sections S2 and S3. During the field campaign, we were able to achieve an average limit of detection (LOD) of 19.4 pptv and limit of quantification (LOQ) of 64.5 pptv for PAN. All PAN data collected during the campaign were well above both limits. Due to the inherently variable sensitivity from this type of instrument, we calibrated three times (start, middle, and end) during the two-month field campaign to confirm instrument stability and consistency of measured PAN. Changes in measurement sensitivity are incorporated into the final calculated PAN mixing ratio to account for any variability in the instrument (see SI for details).

2.3 Generalized Additive Model (GAM) Description

A GAM is used to describe the behavior of the MDA8 O_3 mixing ratios based on meteorological and transport factors at the St. Luke's site in May through September for 2007-2017 (O_3 data at St. Luke's does not start until 2007). The GAM allows us to model a response variable (e.g., MDA8 O_3) based on multiple prediction variables (i.e., meteorological and back-trajectory data) that can have both linear and non-linear effects (Wood, 2017). Camalier et al. (2007) used a similar approach in the eastern U.S. to model O_3 based on meteorological variables and found that this type of model is able to account for the observed variability of O_3 mixing ratios (r^2 = 0.56 - 0.80). They also found that the exact function and optimal meteorological parameters varied by region. Gong et al. (2017) used this approach to characterize the effect of wildfire emissions on MDA8 O_3 in urban areas across the western U.S. By examining the residuals (difference between observed value and model prediction), they found that these results can be used to provide information on abnormal sources of O_3. In particular, they found that on days with wildfire smoke influence, the residuals tend to be high, suggesting an abnormal source of O_3 that cannot be predicted by meteorological or transport variables alone (Gong et al., 2017).

Using methodology similar to Camalier et al. (2007) and Gong et al. (2017), we use GAM results to inform our discussion of wildfire smoke influence on MDA8 O_3 at St. Luke's. We compile 18 meteorological and back-trajectory variables to model MDA8 O_3 using the "mgcv" R package (Wood, 2018). The meteorological variables used are a combination of National Centers for Environmental Prediction (NCEP) Reanalysis data and sounding data from Boise Airport (KBOI), while the transport variables are calculated using the Hybrid Single-Particle Lagrangian Integrated Trajectory (HYSPLIT) model back-trajectories. A full list of variables can be found in Table S2. Details about meteorological and back-trajectory data used to create variables for the GAM can be found in the SI Section S4. We use penalized cubic regression splines to allow non-linearity with each input variable. We customize the variables for Boise to improve our fit, while being careful not to over-fit the model by adjusting knots and examining explanatory values given using the "gam.check" function. We also perform a cross-validation on the GAM model to evaluate performance (see Table S3). Details about choosing parameters, evaluation of overfitting, and cross-validation steps can be found in SI Section S4.4.

2.4 Smoke Criterion

We use the National Oceanic and Atmospheric Administration (NOAA) National Environmental Satellite, Data, and Information Service (NESDIS) Hazard Mapping System (HMS) smoke product and historically averaged PM2.5 thresholds to help identify influence of wildfire smoke. The HMS smoke product uses multiple visible satellite products to identify the presence of smoke at a 4 km spatial resolution one or more times a day. Kaulfus et al. (2017) aggregated HMS data over multiple years and compared this data with ground-based $PM_{2.5}$ concentrations. From this, they found that $PM_{2.5}$ concentrations on HMS-classified smoke vs. non-smoke days have a statistically significant difference, but that the HMS product alone does not always correlate with enhanced PM at the surface. This is because the HMS product does not distinguish between smoke at the ground-level or aloft. Nonetheless, it is still a useful tool in identifying days when wildfire emission might influence pollutants at the surface (Kaulfus et al., 2017). Therefore, we use the HMS smoke product results directly over the St. Luke's site to help determine the influence of wildfire smoke.

In addition to the HMS criteria, we also examine historical $PM_{2.5}$ concentrations for 2006-2017 at St. Luke's. To be certain that wildfire emissions are likely affecting conditions at St. Luke's, we set our $PM_{2.5}$ criteria to the historical daily $PM_{2.5}$ mean (averaged by month) + one standard deviation (σ). Daily (24-hour averaged) $PM_{2.5}$ concentrations are compared to these monthly $PM_{2.5}$ thresholds, which are shown in Table S4. For the hourly $PM_{2.5}$ criterion, we use averaged PM data for 11-17 MST. Figure S2 shows average diurnal PM profiles at St. Luke's for 2006-2017 on smoke and non-smoke days, as defined by the HMS smoke product. We find that regardless of smoke designation, mobile emissions and boundary layer effects contribute to increases in PM during the early morning and late evening. For this reason, we choose to average PM values for 11-17 MST, when PM is less likely to be affected by changes in traffic and boundary layer effects and when O_3 is typically highest. This time period also corresponds to the daily HMS product, providing increased confidence in our smoke or non-smoke designation. From this, the hourly $PM_{2.5}$ criterion is calculated to be 13.6 µg/m^3 (5.7 + 7.9 µg/m^3) using 2006-2017 data for 11-17 MST during August and September. We use these months to calculate the hourly $PM_{2.5}$ criterion to better compare with the 2017 campaign data.

"Smoke" days are defined when both the HMS product shows overhead smoke and the $PM_{2.5}$ concentration is above the designated (hourly or daily) $PM_{2.5}$ criterion. "Non-smoke" days are considered all other cases (only one criteria met, or none). For hourly data, each hour is evaluated against the hourly PM criterion concentration. For daily data, each day is evaluated against the respective daily PM criterion concentration for that particular month.

Because the HMS smoke product is characterized via visible imagery and compiled manually, the product is advertised as a conservative estimate of smoke boundaries that can be attributed to a fixed source (Rolph et al., 2009). Additionally, smoke plumes can be obscured by clouds and hard to distinguish from haze and surface features. Therefore, it is likely that some days show a false negative HMS designation for smoke overhead and our smoke criteria would not be triggered. The calculated PM thresholds for smoke vs. non-smoke conditions may also exclude some smoke days with low $PM_{2.5}$ concentrations. Caveats to both parts of the smoke criterion suggest that the days and hours with smoke present may be misclassified as "no smoke". Thus our wildfire smoke influence should be considered a lower limit. Also, the HMS product does not distinguish between wildland fires and prescribed burning.

2.5 Enhancement Ratios (ERs)

We calculate ERs for $\Delta PM_{2.5}/\Delta CO$, $\Delta NO_y/\Delta CO$, $\Delta PAN/\Delta NO_y$, and $\Delta PAN/\Delta CO$ using hourly summer 2017 data at St. Luke's. These values are obtained by taking the reduced major axis (RMA) regression of two species, with either CO or NO_y on the x-axis. Yokelson et al. (2013) notes that while ERs can be powerful tools to examine different types of pollution phenomena (e.g., wildfire emissions vs. anthropogenic emissions), small changes in these species during mixing with background air can cause significant changes in the calculated ER. This is especially problematic for measurements of plumes that have been transported for more than a day or when the absolute enhancements are relatively small. Therefore, when comparing our calculated ERs with literature values, we consider variability in source emissions and mixing as possible contributors to uncertainty.

3. Results and Discussion

3.1 Summer 2017 Summary Data

Figure 1 shows a typical HMS profile over the northwest U.S. during summer 2017. According to aggregate HMS product analyses done by Brey et al. (2018) and Kaulfus et al. (2017), smoke is frequently seen over Boise. For 2017, Boise had 42 days (out of 61) with HMS smoke overhead between August 1st and September 30th. Additionally, Boise is in an area of increasing $PM_{2.5}$ due to wildfires (McClure and Jaffe, 2018). This makes Boise an ideal location for studying the effect of wildfire smoke in an urban area.

During the 2017 campaign, the St. Luke's site exceeded the NAAQS O_3 standard three times (out of 61 days), while the White Pine site had 10 exceedance days (out of 44 days). The White Pine site O_3 mixing ratios are typically enhanced compared with St. Luke's due to its

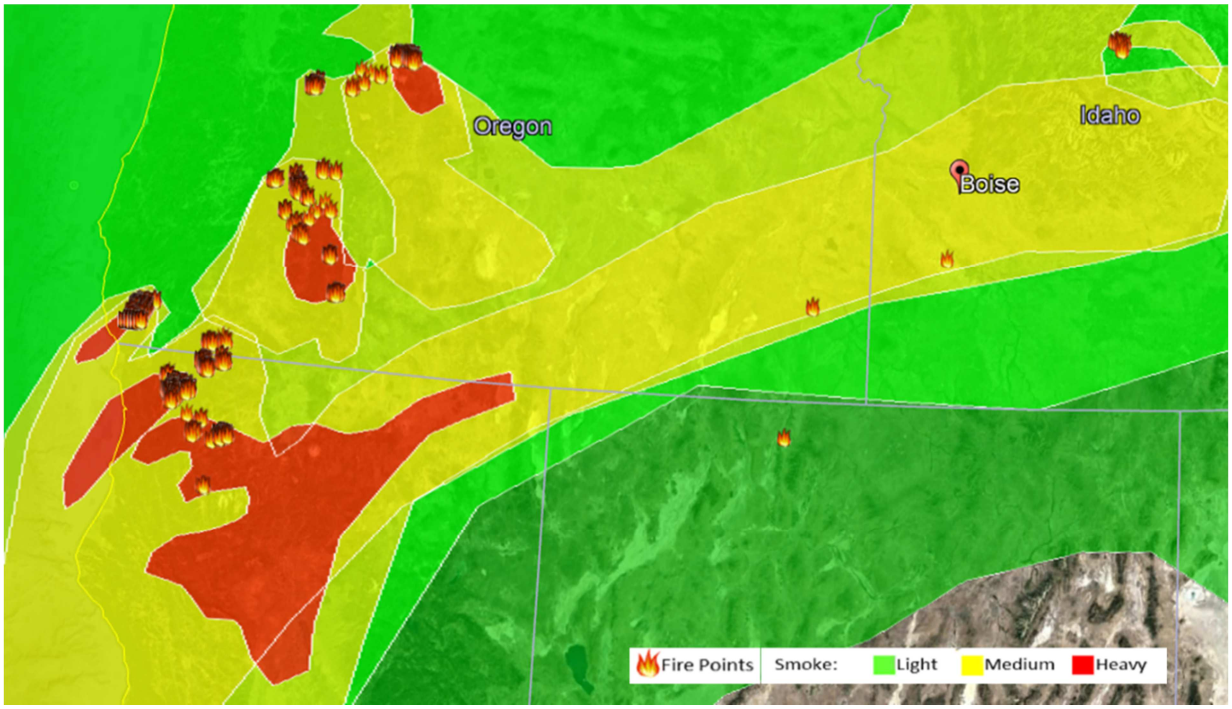

Figure 1. Typical Summer 2017 HMS Smoke Product A typical summer 2017 HMS product map (August 19th) over the northwest U.S. is shown with individual fires and smoke designation in green, yellow, and red. The designations correspond to the HMS estimated smoke densities of 5, 16, and 27 $\mu g/m^3$, respectively. The St. Luke's and White Pine monitoring sites are near Boise, ID.

location downwind of most mobile and industrial emission sources, which emit O_3 precursors, in the Boise area (Kavouras et al., 2008). Throughout the U.S., 2017 had the second most acres burned (less than 1% difference in area burned with record year – 2015) with approximately 68% of the area burned in the western U.S. (NIFC, 2018). Due to the location of Boise, ID, we were able to sample the effect of wildfire smoke in an urban area during one of the highest fire years on record.

Table 1 shows summary statistics for pollutants using daytime (11-17 MST) hourly data during the 2017 summer field campaign at St. Luke's site. Summary information is split between "Non-Smoke" and "Smoke" based on the hourly wildfire criterion detailed in Section 2.4.

Smoke Criteria	PAN (ppbv)	O_3 (ppbv)	$PM_{2.5}$ ($\mu g/m^3$)	NO (ppbv)	NO_y (ppbv)	SO_2 (ppbv)	CO (ppbv)	N Hours
Non-Smoke	**0.739 ± 0.387**	**46.9 ± 13.0**	**8 ± 5**	1.06 ± 0.99	**4.1 ± 3.4**	**0.25 ± 0.15**	**208 ± 63**	225
Smoke	**1.220 ± 0.702**	**60.3 ± 11.1**	**34 ± 28**	1.00 ± 0.93	**5.8 ± 4.2**	**0.40 ± 0.13**	**405 ± 210**	202

Table 1. Boise Summer 2017 Summary Data Daytime (11-17 MST) hourly averages (± 1 σ) for "non-smoke" vs. "smoke" periods during summer 2017 (August 1st – September 30th). The smoke designation is defined by HMS smoke on that day & hourly $PM_{2.5} \geq 13.6$ $\mu g/m^3$. For individual mixing ratios and concentrations, there were 225 "No Fire" hours and 202 "Fire" hours. Bolded values show a statistically significant ($p < 0.05$) difference between smoke and non-smoke days using a 2-tailed t-test.

Bolded compounds show a statistically significant difference between smoke and non-smoke periods (p-value < 0.05). All species are shown to be elevated during smoke hours, except for NO. NO_y values are, on average, 41% higher (1.7 ppbv enhancement) during smoke hours, which implies transport of species crucial for photochemistry into the urban area. PAN mixing ratios are also 65% higher during smoke hours. The average 24-hour temperature during the summer campaign was approximately 22 °C (maximum = 38 °C), which corresponds to an average PAN lifetime of only 2.4 hours (using an average NO_2/NO ratio = 2.4 for back-reaction in polluted areas [NO_x > 100 pptv]) (Roberts, 2007; Zhang et al., 2015). This suggests that PAN is being transported into the area in significant amounts during smoke events and then enters the warm urban photochemical environment where it will have a relatively short lifetime. O_3 mixing ratios also show an enhancement of around 13 ppbv during smoke hours. Figure S3 shows the full diurnal pattern for all compounds listed in Table 1, split between smoke and non-smoke hours. Even though the diurnal patterns in both smoke and non-smoke cases show influence from mobile emissions and boundary layer effects in the early morning/late evening, the daytime enhancements due to the influence of wildfires in the smoke case are clearly visible compared with the non-smoke case.

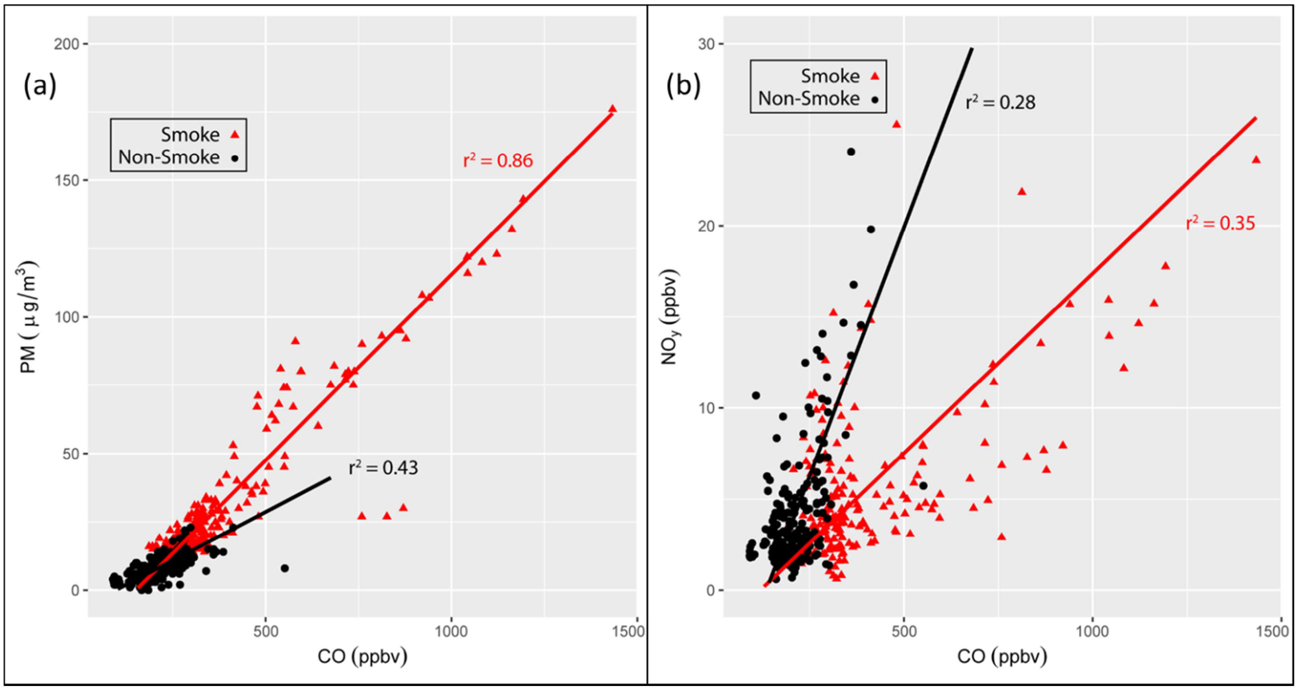

Figure 2. Enhancement Ratios $PM_{2.5}$ vs. CO is shown in plot (a) and NO_y vs. CO is shown in plot (b). Plotted points are hourly data between 11-17 MST for summer 2017 in Boise. "Smoke" hours are shown in red triangles. "Non-smoke" hours are shown in black circles. The smoke designation is defined by HMS smoke on that day & hourly $PM_{2.5} \geq 13.6$ µg/m^3. RMA regression lines are plotted for "smoke" and "non-smoke" designations. All RMA slopes are significant to $p \leq 0.05$ with r^2 values shown next to the regression lines in the representative colors. Slope values associated with these plots are shown in Table 2.

Figure 2 shows hourly PM vs. CO and NO_y vs. CO data during smoke and non-smoke events. RMA regressions of smoke vs. non-smoke events are used to calculate $\Delta PM_{2.5}/\Delta CO$ and $\Delta NO_y/\Delta CO$ ERs based on the slopes. These values can be found in Table 2. In plot (a), smoke hours for $\Delta PM_{2.5}/\Delta CO$ lie predominately along the smoke RMA regression line (red line). A few smoke points can be seen at low PM concentrations and high CO mixing ratios, which occurred during a short rain event. Both regressions show good correlation with few outliers, suggesting that the respective $\Delta PM_{2.5}/\Delta CO$ ERs characterize the smoke vs. non-smoke regimes well. It should be noted that below approximately 25 µg/m^3 of $PM_{2.5}$, it is very difficult to discern which regime $\Delta PM_{2.5}/\Delta CO$ ERs would fall into (smoke vs. non-smoke). In plot (b), non-smoke $\Delta NO_y/\Delta CO$ values predominately fall along the non-smoke RMA regression line (black line).

Smoke Criteria	$\Delta PM_{2.5}/\Delta CO$ ($\mu g/m^3$/ppbv)	$\Delta NO_y/\Delta CO$ (ppbv/ppbv)	$\Delta PAN/\Delta CO$ (ppbv/ppmv)	$\Delta PAN/\Delta NO_y$ (ppbv/ppbv)
No Smoke	0.071 (r^2 = 0.43) (0.064 – 0.079)	0.055 (r^2 = 0.28) (0.049 – 0.061)	NA (r^2 = 0.02)	NA (r^2 = 0.03)
Smoke	0.136 (r^2 = 0.86) (0.129 – 0.144)	0.020 (r^2 = 0.35) (0.018 – 0.022)	3.38 (r^2 = 0.43)	0.171 (r^2 = 0.33)
Laing et al. WF Range	0.092 – 0.164	0.045 – 0.075	NA	NA
EPA WF Range	0.096 – 0.164	0.010 – 0.048	NA	NA

Table 2. Boise Summer 2017 ERs $\Delta PM_{2.5}/\Delta CO$, $\Delta NO_y/\Delta CO$, $\Delta PAN/\Delta CO$, and $\Delta PAN/\Delta NO_y$ ERs are calculated using hourly data between 11-17 MST for summer in Boise during 2017. 95% confidence interval ranges and/or r^2 are shown in parentheses below ERs. The smoke designation is defined by HMS smoke on that day & hourly $PM_{2.5} \geq 13.6$ $\mu g/m^3$. These ERs are calculated using RMA regressions shown in Figures 2 & 3. A NA designation is inserted when data is too variable to provide a useful ER estimate or not available. Laing et al. and EPA Wildfire ER Ranges are taken from Laing et al. (2017).

However, $\Delta NO_y/\Delta CO$ smoke points are more variable. In fact, there are a few smoke points that fall predominately along the non-smoke regression line. It is also possible that some non-smoke points could in fact be smoke points that might be missed by the HMS product, as discussed in Section 2.4. This is likely due to high variance in NO_y values both in the plume and urban background air. We agree with the conclusion by Laing et al. (2017) that $\Delta PM_{2.5}/\Delta CO$ typically shows a significant difference between smoke and non-smoke regimes, while $\Delta NO_y/\Delta CO$ appears to be less reliable in substantiating the influence of wildfire smoke in an urban area.

The $\Delta PM_{2.5}/\Delta CO$ ER in Table 2 for smoke events correspond well with values calculated by Laing et al. (2017) for eight urban sites across the western U.S. Our $\Delta NO_y/\Delta CO$ smoke ER corresponds well with the EPA wildfire range. However, our values for $\Delta NO_y/\Delta CO$ are higher than those provided by Alvarado et al. (2010), Briggs et al. (2016), and DeBell et al. (2004),

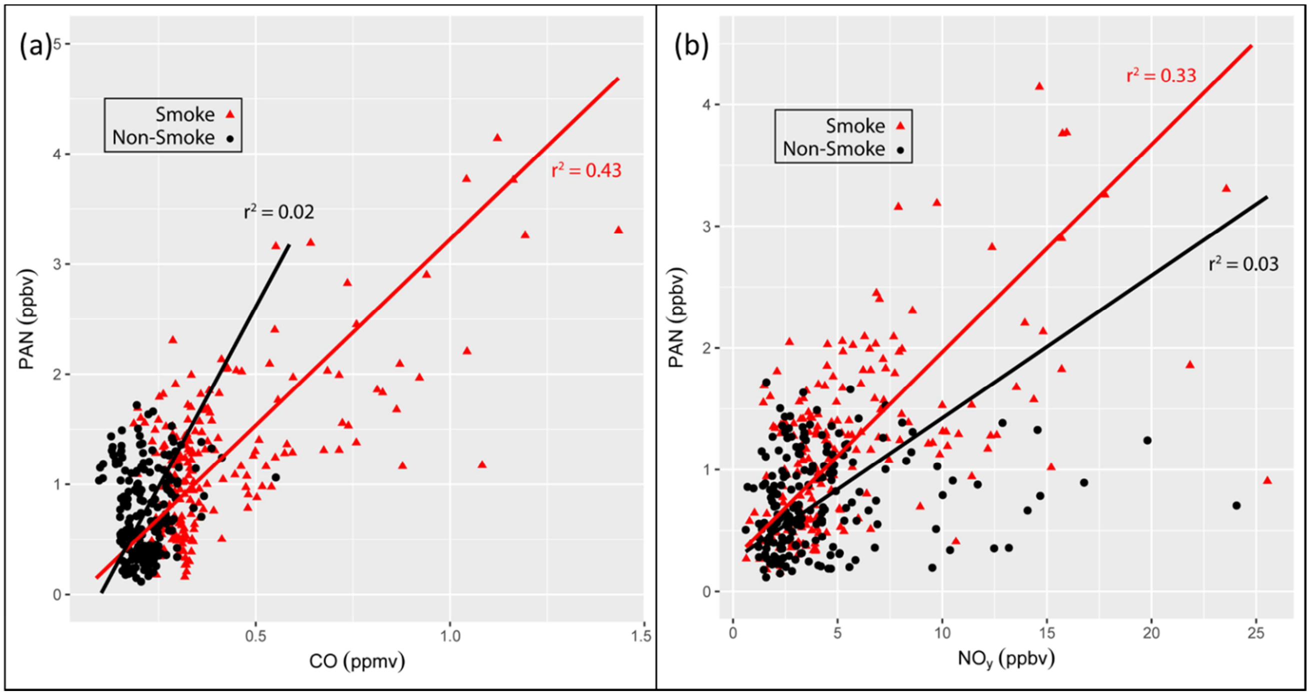

Figure 3. PAN Enhancement Ratios PAN vs. CO is shown in plot (a) and PAN vs. NO_y is shown in plot (b). Plotted points are hourly data between 11-17 MST for summer 2017 in Boise. “Smoke” hours are shown in red triangles. “Non-smoke” hours are shown in black circles. The smoke designation is defined by HMS smoke on that day & hourly $PM_{2.5} \geq 13.6\ \mu g/m^3$. RMA regression lines are plotted for “smoke” and “non-smoke” designations. All RMA slopes show r^2 values next to the regression lines in the representative colors. Slope values associated with these plots are shown in Table 2.

which range from 0.003 to 0.015 ppbv/ppbv. We also suggest that background NO_y and CO values in an urban area would contribute to different $\Delta NO_y/\Delta CO$ ERs compared with samples taken in rural areas (i.e., Alvarado et al. 2010; Briggs et al., 2016; DeBell et al., 2004). No smoke $\Delta NO_y/\Delta CO$ ERs are also substantially lower than urban values from the literature (range = 0.156 – 0.259 ppbv/ppbv); however, this is likely due to literature values being taken in more polluted urban areas (i.e., Houston, TX and Hong Kong) where ratios of NO_y and CO vary significantly due to different anthropogenic emission sources (Mazzuca et al., 2016; Wang et al., 2003).

Figure 3 shows PAN-specific ERs in the same style as Figure 2. Table 2 provides the numerical data associated with Figure 3 for $\Delta PAN/\Delta CO$ and $\Delta PAN/\Delta NO_y$ ERs. Smoke-influenced $\Delta PAN/\Delta CO$ ERs are consistent with literature values given by Briggs et al. (2016) (average = 3.34 ppbv/ppmv) and Alvarado et al. (2010) (range = 2.8 – 3.4 ppbv/ppmv). PAN and CO are uncorrelated on non-smoke days ($r^2 = 0.02$), so an enhancement ratio cannot be derived. Non-smoke $\Delta PAN/\Delta CO$ ERs cannot be used due to low r^2. Similarly, $\Delta PAN/\Delta NO_y$ non-smoke ERs show significant variance and cannot be used reliably. Smoke $\Delta PAN/\Delta NO_y$ ERs show a better correlation but still show variance likely due to variable plume age and processing as it enters the urban area. The overall smoke ER for $\Delta PAN/\Delta NO_y$ shown in Table 2 appears to be lower on average than literature values (we estimate ~0.41 for Briggs et al. (2016)). However, this value is for non-urban environments and does not reflect any influence from anthropogenic combustion sources or higher temperatures at the surface. Also, the PAN and NO_y values reported by Briggs et al. (2016) were significantly lower than our measurements and the PAN percentage of NO_y in wildfire plumes was much higher (Briggs et al. (2016) 25-57% versus our average 12.7%) leading to significantly different $\Delta PAN/\Delta NO_y$ ERs. It should be noted that while we report $\Delta PAN/\Delta CO$ and $\Delta PAN/\Delta NO_y$ ERs here, these values are very different than the $\Delta PM_{2.5}/\Delta CO$ and $\Delta NO_y/\Delta CO$ ERs. While $\Delta PM_{2.5}/\Delta CO$ and $\Delta NO_y/\Delta CO$ ERs can be used in most cases because of their relative stability to determine wildfire or anthropogenic influence, $\Delta PAN/\Delta CO$ and $\Delta PAN/\Delta NO_y$ ERs should be much more variable due to plume photochemical processing, mixing of plume and urban air, and the production of PAN inherent to an urban environment. We expect that $\Delta PAN/\Delta CO$ and $\Delta PAN/\Delta NO_y$ ERs could be used in some cases to determine the influence of wildfire smoke but would generally be highly variable in an urban environment.

Table 3 shows the average daily maximum PAN and MDA8 O_3 values during summer 2017 at St. Luke’s and White Pine sorted by daily smoke criteria. Neither PAN nor $PM_{2.5}$ are

Site	Smoke?	Average Daily Max PAN (ppbv)	Average MDA8 O_3 (ppbv)	Min MDA8 (ppbv)	Max MDA8 (ppbv)	# of Days	# NAAQS Exceedance Days
St. Luke's	No	1.02 ± 0.36	44.4 ± 11.9	25	68	28	0
	Yes	1.71 ± 0.66	58.6 ± 9.3	37	75	33	3
White Pine	No	NA	50.9 ± 13.0	22	73	20	1
	Yes	NA	66.6 ± 6.7	55	76	24	9

Table 3. Boise Summer 2017 Daily Statistics Statistics for daily maximum PAN and MDA8 O_3 in Boise during summer 2017 are shown. Averages are shown with ± 1σ. The smoke designation is defined by HMS smoke on that day & daily $PM_{2.5} \geq$ the historical monthly threshold shown in Table S4. The daily designation of smoke vs. no smoke from St. Luke's was extended to White Pine because $PM_{2.5}$ concentrations are not measured at White Pine.

measured at the White Pine site. To determine smoke vs. non-smoke days at White Pine, we assume the same daily designation used for St. Luke's. At the St. Luke's site, daily maximum PAN is 68% higher (0.69 ppbv) on smoke days compared with non-smoke days. On average, MDA8 O_3 values are also enhanced by approximately 32% and 31% on smoke versus non-smoke days at St. Luke's and White Pine, respectively. The highest non-smoke day does not exceed the NAAQS standard for O_3 at St. Luke's, while only one non-smoke day exceeds the standard at White Pine. On smoke days, the NAAQS is exceeded on three days at St. Luke's and nine days at White Pine. This is consistent with the assertion by Kaulfus et al. (2017) that the influence of wildfire smoke can significantly affect compliance with the O_3 standard.

3.2 Particulate Matter Influence on Ozone Production

Previously, it has been suggested that PM may have a significant positive or negative effect on O_3 production due to the forward/backward scattering and/or absorption of solar radiation (Alvarado et al., 2015; Baylon et al., 2018; Real et al., 2007; Reid et al., 2005). To investigate this assertion, we use historical $PM_{2.5}$ concentrations versus MDA8 O_3 from the St. Luke's site during all months for 2007-2017. Figure 4 shows MDA8 O_3 binned by 24-hour averaged $PM_{2.5}$ in the top row and daytime (11-17 MST) averaged $PM_{2.5}$ in the bottom row. Days are separated based solely on the HMS designation (no smoke versus smoke overhead). While this may not explicitly characterize smoke at the surface, Kaulfus et al. (2017) suggests that we are able to determine when the surface is potentially affected by smoke and shows a statistically significant difference in surface-level $PM_{2.5}$ between HMS smoke and non-smoke days. Specifically at the St. Luke's site, $PM_{2.5}$ concentrations for May-September on HMS smoke and non-smoke days are 14.3 and 7.0 $\mu g/m^3$, respectively, and these distributions are statistically different (p-value < 0.01). Based on Figure 4, we determine that MDA8 O_3 generally decreases with increasing $PM_{2.5}$ on non-smoke days. We suggest that this is due to NO_x-titration of O_3 at high PM levels. Figure 5 shows NO binned by 24-hour and daytime average $PM_{2.5}$, comparable with of Figure 4, for 2011-2017 at St. Luke's (NO data is not available before 2011). These plots show that for non-smoke days, at $PM_{2.5}$ concentrations above approximately 20 $\mu g/m^3$, we see significant enhancements in NO mixing ratios compared with smoke days.

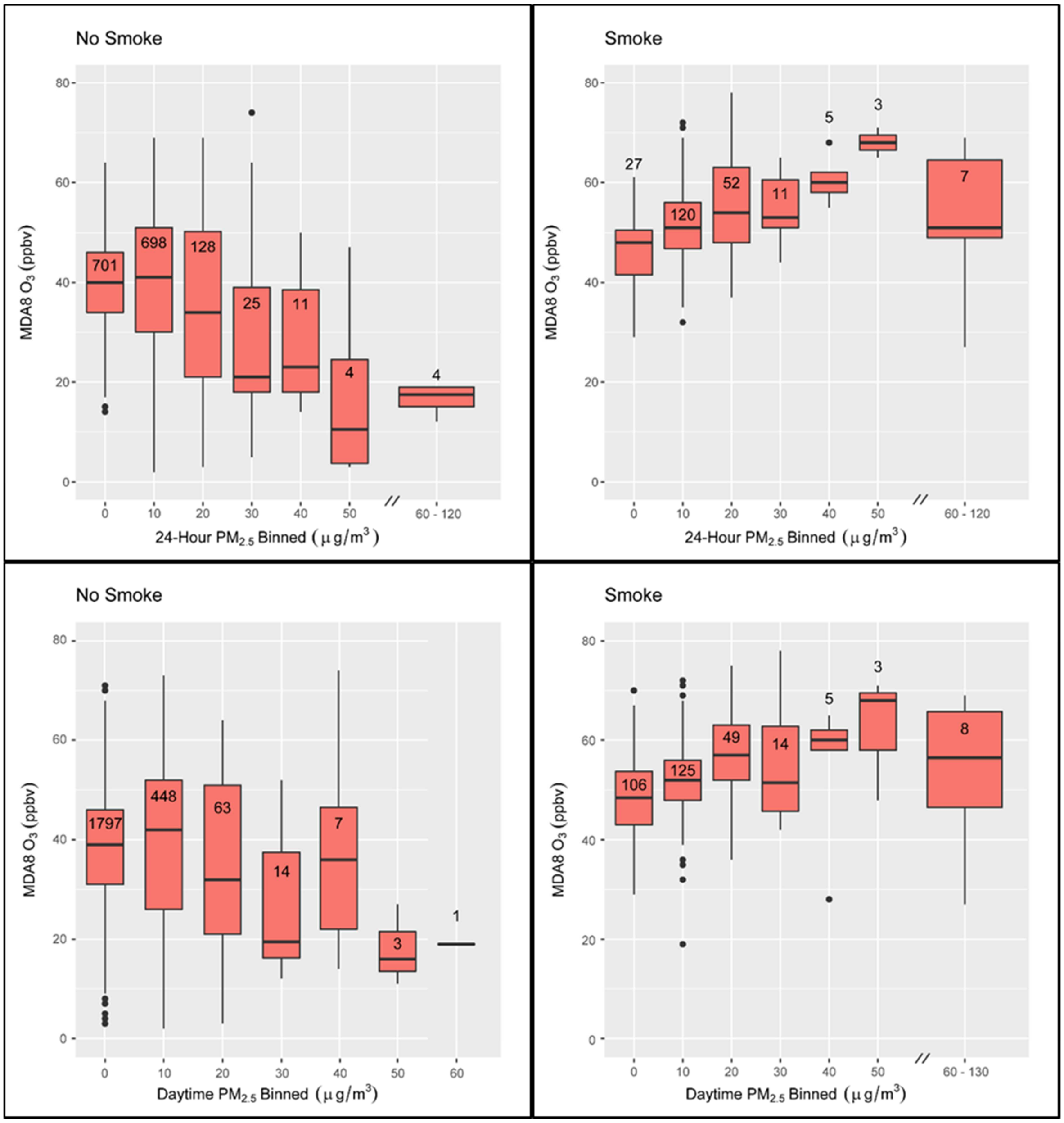

Figure 4. Box Plots of MDA8 O_3 binned by $PM_{2.5}$ All months MDA8 O_3 data for 2007-2017 is split by HMS criteria. Plots (a) and (b) show MDA8 O_3 binned by 24-hour average $PM_{2.5}$ (using daily data). Plots (c) and (d) show MDA8 O_3 binned by daytime (11-17 MST) average $PM_{2.5}$ (using hourly data). Plots (a) and (c) are periods with "no smoke"; plots (b) and (d) are periods with "smoke" according to the HMS smoke product only. Each bin includes the designated $PM_{2.5}$ values ± 5 μg/m^3.

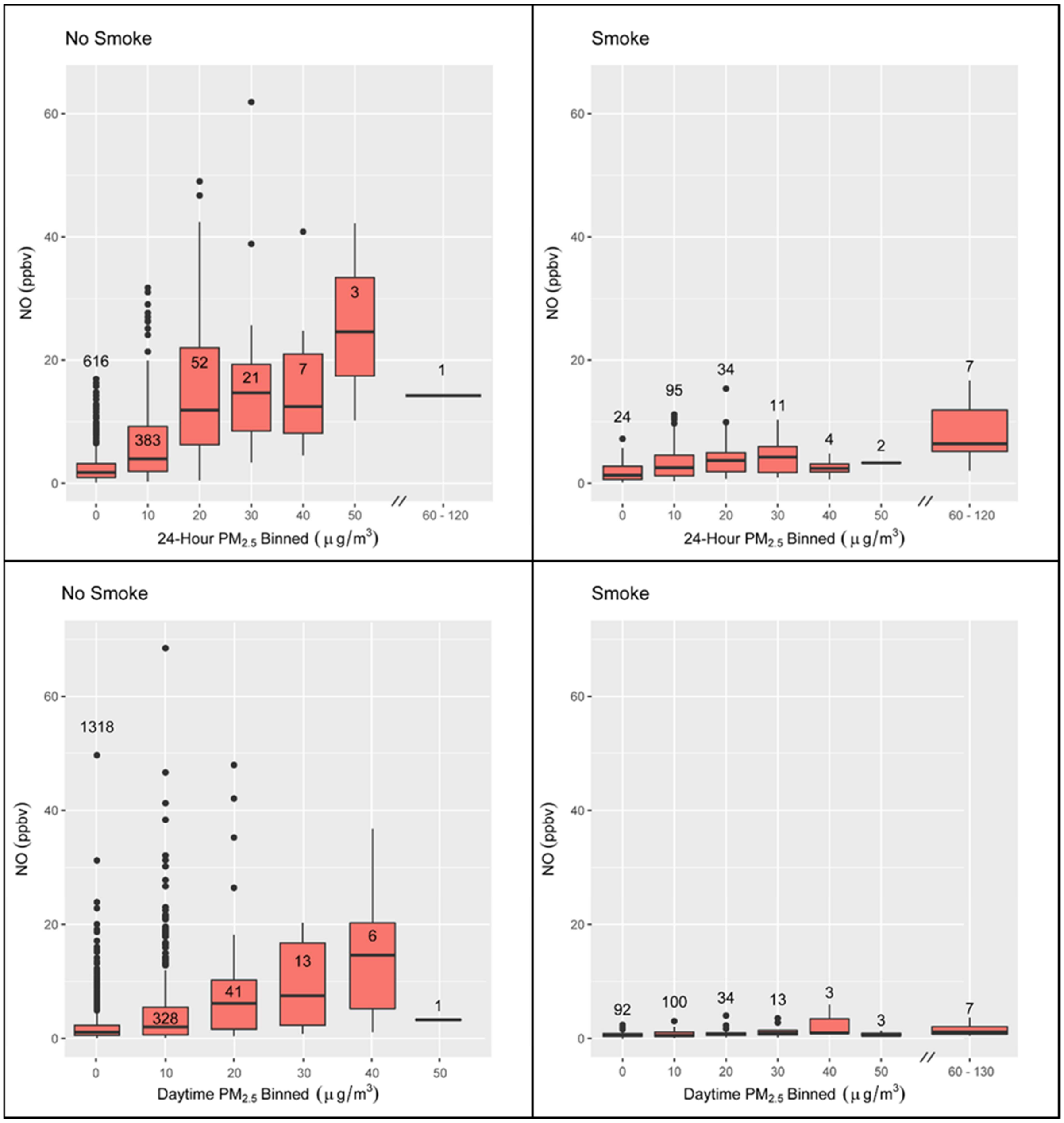

Figure 5. Box Plots of NO binned by $PM_{2.5}$ All months NO data (2011-2017) is split by HMS criteria. Plots (a) and (b) show NO binned by 24-hour average $PM_{2.5}$ (using daily data). Plots (c) and (d) show NO binned by daytime (11-17 MST) average $PM_{2.5}$ (using hourly data). Plots (a) and (c) are periods with "no smoke"; plots (b) and (d) are periods with "smoke" according to the HMS smoke product only. Each bin includes the designated $PM_{2.5}$ values ± 5 $\mu g/m^3$.

For MDA8 O_3 on smoke days (plots (b) and (d) in Figure 4), we see MDA8 O_3 increasing with increasing $PM_{2.5}$ up to approximately 60-70 $\mu g/m^3$. After this point, MDA8 O_3 is, on average, lower at very high $PM_{2.5}$ concentrations. This suggests that at sufficiently high $PM_{2.5}$ concentration, O_3 production can be suppressed, likely due to back-scattering of solar radiation or very young plume age. These observations extend the modelling done by Baylon et al. (2018) and Alvarado et al. (2015) to higher concentration of $PM_{2.5}$ and provides important context for decreased O_3 production in urban areas under very high levels of smoke.

3.3 St. Luke's GAM Results

Table 4 shows summary statistics from the GAM simulation of MDA8 O_3 at St. Luke's during May through September for 2007-2017. We use residuals (similar to Camalier et al. (2007) and Gong et al. (2017)) to identify variations in MDA8 O_3 that cannot be predicted by the meteorological or transport variables(listed in Table S2). Overall, we see a low average and standard deviation for all residuals in addition to a moderate r^2 value. This

Months Used	Smoke Day Residuals (ppbv)	Non-Smoke Day Residuals (ppbv)	Residual 95^{th} Percentile (ppbv)	Residual 97.5^{th} Percentile (ppbv)	r^2	N variables
May-Sep	4.93 ± 6.89 (n = 78)	0.00 ± 5.68 (n = 872)	9.15	11.4	0.57	15

Table 4. GAM Summary Statistics GAM results are shown for the St. Luke's site during 2007-2017. Average for smoke and non-smoke day GAM MDA8 O_3 residuals are shown with $\pm 1\sigma$ and number of data points. The 95^{th} and 97.5^{th} percentiles of the residuals are calculated using non-smoke day data. The smoke designation is defined by HMS smoke on that day & daily $PM_{2.5} \geq$ the historical monthly threshold shown in Table S4.

suggests that the model was able to fit MDA8 O_3 mixing ratios reasonably well given the input variables. While only 4% of days are classified as smoke days (using the daily smoke criterion), they show significantly higher residuals than non-smoke days (residuals = 4.93 ppbv vs. 0.00 ppbv, respectively), suggesting that the enhancement in O_3 on smoke days is not associated with standard meteorology or transport variables. The mean smoke day residual for St. Luke's is slightly larger than the same value (3.2 ppb) determined for Boise by Gong et al. (2017) using a very similar method. The most likely cause for this difference is that our values are based on the non-smoke GAMs, thus this gives the full influence of smoke on the MDA8 O_3, whereas in Gong's analysis, all days were included in the GAMs. Figure 6 shows Observed MDA8 O_3 versus GAM Fit MDA8 O_3 separated by the smoke and non-smoke criteria. Smoke values (in red triangles) show a higher tendency to be well above or below the 1:1 line. We also calculate 95th and 97.5th percentile residual values (9.66 ppbv & 11.7 ppbv, respectively) to help identify days when outside sources (i.e., sources not included as explanatory variables in the GAM) make significant contributions to MDA8 O_3. This can be used to support exceptional event classification (Gong et al., 2017). Figure S4 shows the GAM smoke residuals plotted versus ΔPM (defined as average monthly, "non-smoke" $PM_{2.5}$ subtracted from the 24-hour average $PM_{2.5}$) for May through September in 2007-2017. This figure shows a similar result compared to Figure 4, with GAM residuals increasing up to $PM_{2.5}$ concentrations of approximately 60 $\mu g/m^3$ then decreasing at very high $\Delta PM_{2.5}$ concentrations. Figure S5 shows the GAM residuals binned by GAM Fit O_3 values. This figure shows that the average residual is approximately zero for each bin. Additionally, for GAM-predicted O_3 values between 60 and 80 ppbv, we find an average residual of 1.04 ± 3.90 ppbv (n = 13) and 8.12 ± 10.3 ppbv (n = 3), for non-smoke and smoke days, respectively. The fact that the smoke residuals are higher at the higher mixing ratios indicates a tendency for greater smoke impacts on O_3 on more photochemically active days.

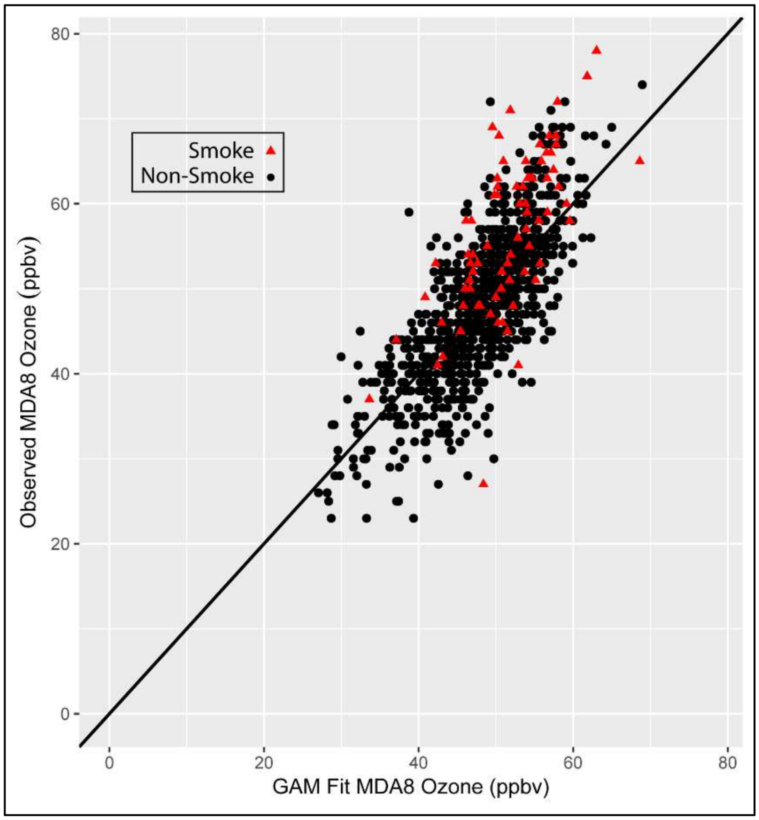

Figure 6. Boise Observed MDA8 O_3 vs. GAM Fit MDA8 O_3
Daily May-September for 2007-2017 GAM MDA8 O_3 results are plotted versus Observed MDA8 O_3 for Boise. The smoke designation is defined by HMS smoke on that day & daily $PM_{2.5}$ ≥ the historical monthly threshold. “Smoke” data (n = 78) is shown in red and “non-smoke” data (n = 872) is shown in black. The black line is 1:1.

3.4 Wildfire Smoke Enhanced O_3 Events during Summer 2017

Summary data for the four highest MDA8 O_3 events during summer 2017 (August 1^{st} – September 30^{th}) at St. Luke’s are listed in Table 5. All events were classified as smoke influenced by the HMS smoke product and daily PM criteria. Three of these days had MDA8 O_3 values >0.07 ppm. $\Delta PM_{2.5}/\Delta CO$ and $\Delta NO_y/\Delta CO$ values can be compared with smoke vs. non-smoke ERs in Table 2. GAM residual values should be compared with the 95^{th} and 97.5^{th} percentile thresholds in Table 4. Table S3 shows data for each day during summer 2017, comparable with Table 5.

Date	MDA8 O_3 (ppbv)	24-Hr Avg. $PM_{2.5}$ ($\mu g/m^3$)	Daily Max PAN (ppbv)	$\Delta PM_{2.5}/\Delta CO$ ($\mu g/m^3$/ppbv)	$\Delta NO_y/\Delta CO$ (ppbv/ppbv)	GAM Residual (ppbv)
Aug. 2nd	75	18	2.31	0.114 ($r^2 = 0.21$)	0.067 ($r^2 = 0.67$)	13.2
Aug. 6th	69	69	2.40	0.223 ($r^2 = 0.96$)	0.038 ($r^2 = 0.02$)	19.4
Aug. 27th	72	22	1.32	-0.108 ($r^2 = 0.00$)	0.039 ($r^2 = 0.53$)	14.0
Sept. 5th	47	76	2.45			-2.3
Sept. 6th	51	120	4.14	0.138 ($r^2 = 0.97$)	0.021 ($r^2 = 0.61$)	-4.2
Sept. 7th	51	87	2.05			-0.8
Sept. 8th	71	42	3.19			19.1

Table 5. Boise Summer 2017 Wildfire-Influenced Events Four of the highest O_3 events occurring in Boise during summer 2017 are shown. August 2nd, 6th, and 27th are single-day events. September 5th – 8th is a multi-day wildfire event. $\Delta PM_{2.5}/\Delta CO$ and $\Delta NO_y/\Delta CO$ values are calculated using data from 11-17 MST. GAM residual values are also provided for comparison with Table 4.

August 2nd and 27th show moderate $PM_{2.5}$ concentrations. Figure 7 shows the event on August 2nd, 2017 and enhanced O_3. Both days are designated as smoke days due to their enhanced PM and HMS smoke. Figure S6 shows the event on August 27th, 2017. During these events, $\Delta PM_{2.5}/\Delta CO$ and $\Delta NO_y/\Delta CO$ ERs exhibit a wide range of values and some are outside of the typical wildfire range (as shown in Table 2). While we know that these events are influenced by wildfire smoke (high PM, O_3, back-trajectories identify fires, smoke overhead, etc.), we find that these ERs have a very wide range during smoke days in an urban area which likely reflects mixing with urban emissions. Looking back at Figure 2 (a), it is difficult to distinguish between smoke and non-smoke $\Delta PM_{2.5}/\Delta CO$ ERs at $PM_{2.5}$ concentrations below 25 $\mu g/m^3$. We suggest that for these events, which both have transport times of one to two days (as estimated by HYSPLIT back-trajectories); enhancements of $PM_{2.5}$ are typically low due to cloud processing or deposition (Wigder et al., 2013). Additionally, Figure 2 (b) also shows that smoke vs. non-smoke

$\Delta NO_y/\Delta CO$ ERs are difficult to distinguish at low NO_y and CO mixing ratios. We suggest that as wildfire smoke influence increases, ERs become more useful in determining smoke days from non-smoke days.

For these two events, we are able to confirm the influence of wildfire smoke by using the $PM_{2.5}$, CO and PAN enhancements and back-trajectories. Back-trajectories for both events (see Figures S7 & S8) show transport over wildfires in southwest Oregon and northern California.

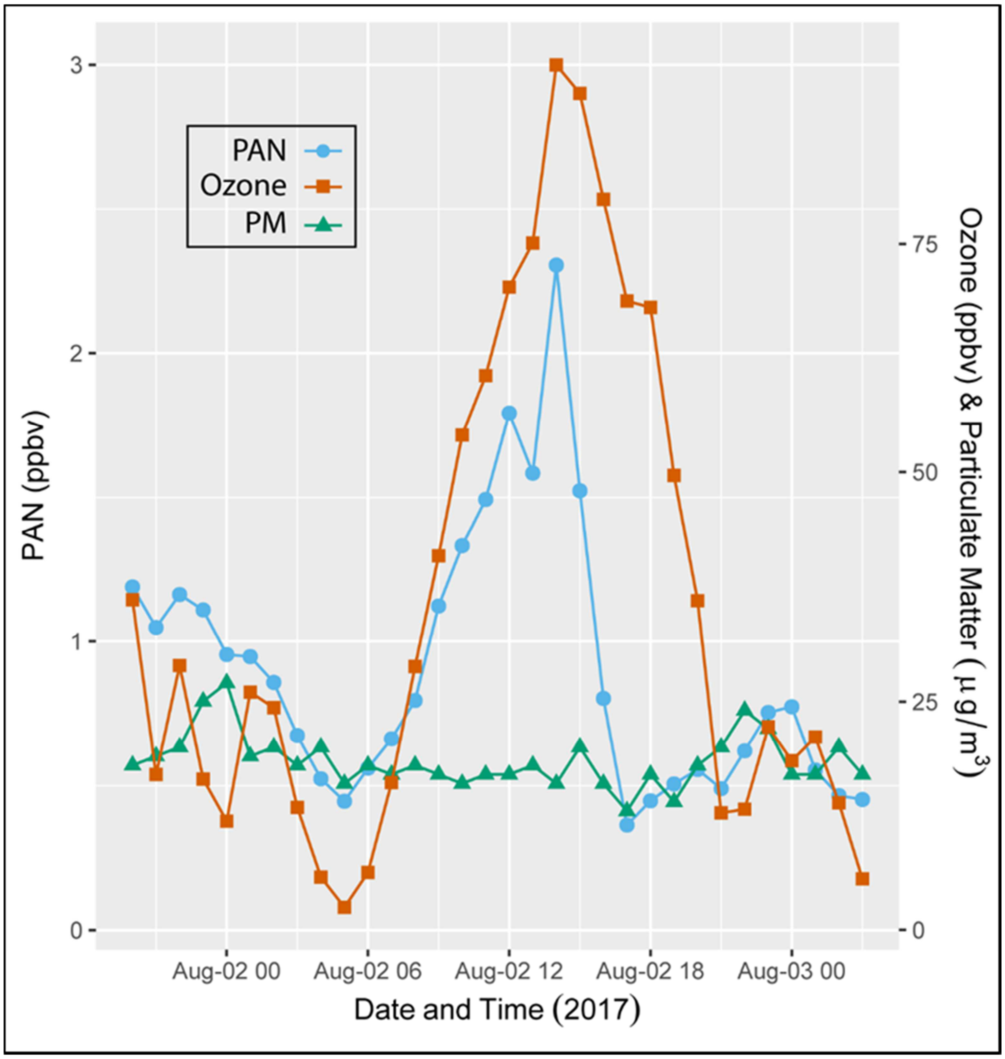

Figure 7. August 2nd, 2017 Wildfire-Influenced Event A moderate $PM_{2.5}$, high PAN and O_3 wildfire-influenced smoke day is shown. PAN, O_3, and $PM_{2.5}$ data are shown in blue, orange, and green, respectively. All values are hourly averages. Dates and times are in MST.

Along these back-trajectories, temperatures are low enough for the PAN lifetime to be approximately 1-1.5 days (total transport time ~1.5 days). The air masses then descend into the warmer boundary layer in the Boise area due to high pressure circulation. This would allow storage of PAN during transport, then loss of PAN back to NO_x as the air mass enters the Boise area, which could enhance O_3 production on these days. Daily maximum PAN mixing ratios are also consistent with smoke day values shown in Table 1. Additionally, GAM residuals are above the 95th percentile threshold for both days, suggesting an anomalous source of O_3, which we attribute to the influence of wildfire smoke. At the same time, for moderate smoke days such as those described, additional data or observations would help confirm the presence of wildfire smoke.

Figure 8 shows the time series of a very high smoke event (high $PM_{2.5}$, O_3, PAN, and CO) observed at the St. Luke's site during the period of September 6th – 8th, 2017. The HMS smoke product shows the whole northwest U.S. blanketed in smoke for this entire period. During the first three days of this event (September 5th – 7th), $PM_{2.5}$ concentrations are consistently above 70 $\mu g/m^3$. During this time, MDA8 O_3 values do not appear to be significantly enhanced and GAM residuals even show a small overestimate of the observed MDA8 O_3 (negative values). However, when $PM_{2.5}$ concentrations drop below 70 $\mu g/m^3$ on the fourth day of the event (Sept. 8th), we see a 20 ppbv increase in MDA8 O_3. We also see a significant underestimation of observed MDA8 values by the GAM model, which shows a residual of 19.1 ppbv that exceeds both the 95th and 97.5th percentile thresholds. This suggests significant anomalous influences not captured by the GAM model. We assert that during the first three days of the event, $PM_{2.5}$ concentrations were sufficiently high enough to impede O_3 production, consistent with the conclusions drawn from Figure 4. On the fourth day, $PM_{2.5}$ concentrations had dropped somewhat so that O_3 was able to be produced efficiently. This led to an MDA8 O_3 value of 71 ppbv. During this event, we observe one to two day transport times via back-trajectories. It is possible, however, that the low O_3 production on September 5-7th is due to the plumes being fairly young. PAN values peak during the highest smoke concentrations, likely due to wildfire plume transport into the area. On the fourth day, PAN and O_3 increase significantly during the day due to photochemical production with PAN mixing ratios at almost two times the daily smoke average. Both $\Delta PM_{2.5}/\Delta CO$ and $\Delta NO_y/\Delta CO$ ERs during this multi-day event are clearly indicative of wildfire smoke.

In contrast, August 6th shows an example of a high O_3 smoke event where the 24-hour average $PM_{2.5}$ concentration was 69 µg/m^3. While Figure 4 would suggest that we might see a reduction in O_3 production, we actually see an MDA8 O_3 level of 69 ppbv. This demonstrates the complexity and large variability associated with O_3 production from wildfire plumes in urban areas. This contrasting event suggests that the threshold for O_3 enhancement and suppression is uncertain in the range of $PM_{2.5}$ concentrations between 60 and 70 µg/m^3.

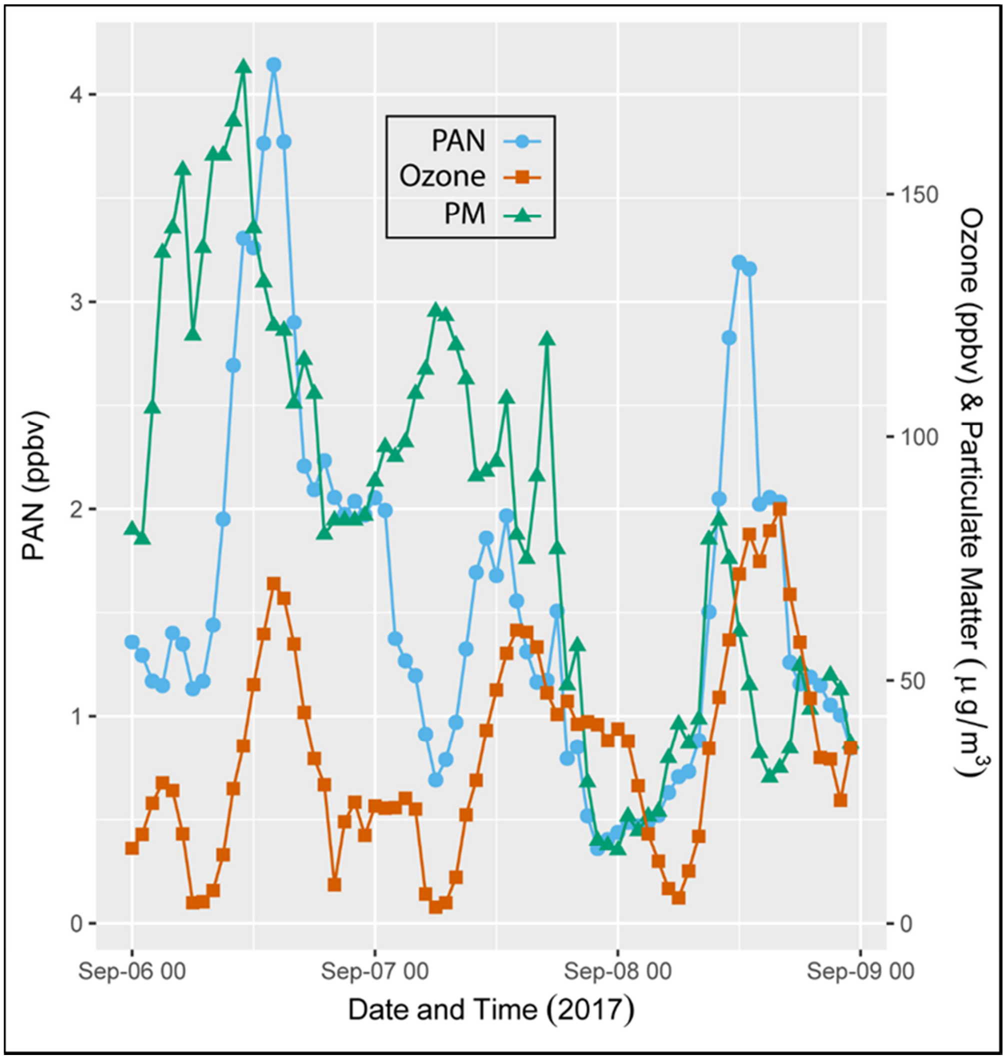

Figure 8. September 6th-8th, 2017 Wildfire-Influenced Event A multi-day high $PM_{2.5}$, PAN, and O_3 wildfire-influenced smoke event is shown. PAN, O_3, and $PM_{2.5}$ data are shown in blue, orange, and green, respectively. All values are hourly averages. Dates and times are in MST.

4. Conclusions

During the 2017 intensive campaign at the St. Luke's site, we determined that all individual pollutants measured were significantly enhanced during smoke days compared with non-smoke days, with the exception of NO. Additionally, we found that MDA8 O_3 and daily maximum PAN mixing ratios were 32% and 68% higher on smoke days, respectively. Using historical data from the St. Luke's site during 2007-2017, we show that MDA8 O_3 decreases with increasing $PM_{2.5}$ on non-smoke days, likely due to NO_x-titration. On smoke days, MDA8 O_3 increases with increasing $PM_{2.5}$ up to a threshold (~ 60 – 70 µg/m^3), at which point MDA8 O_3 is (on average) lower during very high smoke events. We use GAM residual values to determine anomalous sources of O_3 that cannot be predicted by meteorological or transport variables. Based on these results, we find that smoke day residuals are significantly higher than non-smoke day residuals. We also investigate four wildfire-influenced, high O_3 events. These cases show that ERs become more useful as smoke concentrations increase, and the threshold between O_3 enhancement and suppression for Boise is in the range of 60 – 70 µg/m^3. While we identify some effects on O_3 due to wildfire emissions in an urban area, the need for improved classification of smoke versus non-smoke influenced days will likely become more important throughout the western U.S. as wildfire frequency and intensity are predicted to increase through the end of the century.

Acknowledgements

We would like to thank Rick Hardy, Ed Jolly, Steve Miller, Kimi Smith, Mary Walsh, and the Idaho Department of Environmental Quality for allowing us to take PAN measurements at the St. Luke's site, providing data, reviewing this article, and assistance during the field campaign. We also acknowledge Larry Oolman at the University of Wyoming for providing sounding data. Additionally, we would like to thank Aaron Kaulfus for suppling HMS smoke data for the St. Luke's site. Funding for this research was provided by the National Science Foundation (#1447832) and the National Oceanic and Atmospheric Administration (#NA17OAR431001).

References

Akagi, S.K., Yokelson, R.J., Burling, I.R., Meinardi, S., Simpson, I., Blake, D.R., McMeeking, G.R., Sullivan, A., Lee, T., Kreidenweis, S., Urbanski, S., Reardon, J., Griffith, D.W.T., Johnson, T.J., Weise, D.R., 2013. Measurements of reactive trace gases and variable O_3 formation rates in some South Carolina biomass burning plumes. Atmospheric Chem. Phys. 13, 1141–1165. https://doi.org/10.5194/acp-13-1141-2013

Akagi, S.K., Yokelson, R.J., Wiedinmyer, C., Alvarado, M.J., Reid, J.S., Karl, T., Crounse, J.D., Wennberg, P.O., 2011. Emission factors for open and domestic biomass burning for use in atmospheric models. Atmos Chem Phys 11, 4039–4072. https://doi.org/10.5194/acp-11-4039-2011

Aldersley, A., Murray, S.J., Cornell, S.E., 2011. Global and regional analysis of climate and human drivers of wildfire. Sci. Total Environ. 409, 3472–3481. https://doi.org/10.1016/j.scitotenv.2011.05.032

Alvarado, M., Logan, J., Mao, J., Apel, E., Riemer, D., Blake, D., Cohen, R., Min, K.-E., Perring, A., Browne, E., 2010. Nitrogen oxides and PAN in plumes from boreal fires during ARCTAS-B and their impact on ozone: an integrated analysis of aircraft and satellite observations. Atmospheric Chem. Phys. 10, 9739–9760.

Alvarado, M., Lonsdale, C., Yokelson, R., Akagi, S.K., Coe, H., Craven, J., Fischer, E., McMeeking, G., Seinfeld, J., Soni, T., 2015. Investigating the links between ozone and organic aerosol chemistry in a biomass burning plume from a prescribed fire in California chaparral. Atmospheric Chem. Phys. 15, 6667–6688.

Balch, J.K., Bradley, B.A., Abatzoglou, J.T., Nagy, R.C., Fusco, E.J., Mahood, A.L., 2017. Human-started wildfires expand the fire niche across the United States. Proc. Natl. Acad. Sci. 114, 2946–2951.

Baylon, P., Jaffe, D., Hall, S., Ullmann, K., Alvarado, M., Lefer, B., 2018. Impact of Biomass Burning Plumes on Photolysis Rates and Ozone Formation at the Mount Bachelor Observatory. J. Geophys. Res. Atmospheres 123, 2272–2284.

Baylon, P., Jaffe, D.A., Wigder, N.L., Gao, H., Hee, J., 2015. Ozone enhancement in western US wildfire plumes at the Mt. Bachelor Observatory: The role of NOx. Atmos. Environ. 109, 297–304. https://doi.org/10.1016/j.atmosenv.2014.09.013

Baylon, P.M., Jaffe, D.A., Pierce, R.B., Gustin, M.S., 2016. Interannual Variability in Baseline Ozone and Its Relationship to Surface Ozone in the Western U.S. Environ. Sci. Technol. 50, 2994–3001. https://doi.org/10.1021/acs.est.6b00219

Brey, S.J., Ruminski, M., Atwood, S.A., Fischer, E.V., 2018. Connecting smoke plumes to sources using Hazard Mapping System (HMS) smoke and fire location data over North America. Atmospheric Chem. Phys. 18, 1745–1761.

Briggs, N.L., Jaffe, D.A., Gao, H., Hee, J.R., Baylon, P.M., Zhang, Q., Zhou, S., Collier, S.C., Sampson, P.D., Cary, R.A., 2016. Particulate matter, ozone, and nitrogen species in aged wildfire plumes observed at the Mount Bachelor Observatory. Aerosol Air Qual Res 16, 3075–3087.

Camalier, L., Cox, W., Dolwick, P., 2007. The effects of meteorology on ozone in urban areas and their use in assessing ozone trends. Atmos. Environ. 41, 7127–7137. https://doi.org/10.1016/j.atmosenv.2007.04.061

Castro, T., Madronich, S., Rivale, S., Muhlia, A., Mar, B., 2001. The influence of aerosols on photochemical smog in Mexico City. Atmos. Environ. 35, 1765–1772.

DeBell, L.J., Talbot, R.W., Dibb, J.E., Munger, J.W., Fischer, E.V., Frolking, S.E., 2004. A major regional air pollution event in the northeastern United States caused by extensive forest fires in Quebec, Canada. J. Geophys. Res. Atmospheres 109.

Dennison, P.E., Brewer, S.C., Arnold, J.D., Moritz, M.A., 2014. Large wildfire trends in the western United States, 1984–2011. Geophys. Res. Lett. 41, 2928–2933. https://doi.org/10.1002/2014GL059576

Fischer, E.V., Jaffe, D.A., Reidmiller, D.R., Jaegle, L., 2010. Meteorological controls on observed peroxyacetyl nitrate at Mount Bachelor during the spring of 2008. J. Geophys. Res. Atmospheres 115.

Flocke, F.M., Weinheimer, A.J., Swanson, A.L., Roberts, J.M., Schmitt, R., Shertz, S., 2005. On the measurement of PANs by gas chromatography and electron capture detection. J. Atmospheric Chem. 52, 19–43.

Gong, X., Kaulfus, A., Nair, U., Jaffe, D.A., 2017. Quantifying O3 Impacts in Urban Areas Due to Wildfires Using a Generalized Additive Model. Environ. Sci. Technol. 51, 13216–13223. https://doi.org/10.1021/acs.est.7b03130

Hallar, A.G., Molotch, N.P., Hand, J.L., Livneh, B., McCubbin, I.B., Petersen, R., Michalsky, J., Lowenthal, D., Kunkel, K.E., 2017. Impacts of increasing aridity and wildfires on aerosol loading in the intermountain Western US. Environ. Res. Lett. 12. https://doi.org/10.1088/1748-9326/aa510a

Honrath, R., Owen, R.C., Val Martin, M., Reid, J., Lapina, K., Fialho, P., Dziobak, M.P., Kleissl, J., Westphal, D., 2004. Regional and hemispheric impacts of anthropogenic and biomass burning emissions on summertime CO and O3 in the North Atlantic lower free troposphere. J. Geophys. Res. Atmospheres 109.

Jaffe, D., Chand, D., Hafner, W., Westerling, A., Spracklen, D., 2008a. Influence of Fires on O3 Concentrations in the Western U.S. Environ. Sci. Technol. 42, 5885–5891. https://doi.org/10.1021/es800084k

Jaffe, D., Hafner, W., Chand, D., Westerling, A., Spracklen, D., 2008b. Interannual Variations in PM2.5 due to Wildfires in the Western United States. Environ. Sci. Technol. 42, 2812–2818. https://doi.org/10.1021/es702755v

Jaffe, D.A., Wigder, N.L., 2012. Ozone production from wildfires: A critical review. Atmos. Environ. 51, 1–10. https://doi.org/10.1016/j.atmosenv.2011.11.063

Jiang, X., Wiedinmyer, C., Carlton, A.G., 2012. Aerosols from fires: An examination of the effects on ozone photochemistry in the Western United States. Environ. Sci. Technol. 46, 11878–11886.

Kaulfus, A.S., Nair, U., Jaffe, D., Christopher, S.A., Goodrick, S., 2017. Biomass Burning Smoke Climatology of the United States: Implications for Particulate Matter Air Quality. Environ. Sci. Technol. 51, 11731–11741. https://doi.org/10.1021/acs.est.7b03292.

Kavouras, I.G., DuBois, D.W., Etyemezian, V., Nikolich, G., Louks, B., 2008. Ozone and its precursors in the Treasure Valley, Idaho. Dep. Environ. Qual. State Ida.

Kitzberger, T., Brown, P.M., Heyerdahl, E.K., Swetnam, T.W., Veblen, T.T., 2007. Contingent Pacific–Atlantic Ocean influence on multicentury wildfire synchrony over western North America. Proc. Natl. Acad. Sci. 104, 543–548. https://doi.org/10.1073/pnas.0606078104

Laing, J.R., Jaffe, D.A., Hee, J.R., 2016. Physical and optical properties of aged biomass burning aerosol from wildfires in Siberia and the Western USA at the Mt. Bachelor Observatory. Atmospheric Chem. Phys. 16, 15185–15197. https://doi.org/10.5194/acp-16-15185-2016

Laing, J.R., Jaffe, D.A., Slavens, A.P., Li, W., Wang, W., 2017. Can ΔPM2.5/ΔCO and ΔNOy/ΔCO Enhancement Ratios Be Used to Characterize the Influence of Wildfire Smoke in Urban Areas? Aerosol Air Qual. Res. 17, 2413–2423. https://doi.org/10.4209/aaqr.2017.02.0069

Littell, J.S., McKenzie, D., Peterson, D.L., Westerling, A.L., 2009. Climate and wildfire area burned in western U.S. ecoprovinces, 1916–2003. Ecol. Appl. 19, 1003–1021. https://doi.org/10.1890/07-1183.1

Lu, X., Zhang, L., Xu, Y., Zhang, J., Jaffe, D.A., Stohl, A., Zhao, Y., Shao, J., 2016. Wildfire influences on the variability and trend of summer surface ozone in the mountainous western United States. Atmospheric Chem. Phys. 16, 14687.

Mazzuca, G.M., Ren, X., Loughner, C.P., Estes, M., Crawford, J.H., Pickering, K.E., Weinheimer, A.J., Dickerson, R.R., 2016. Ozone production and its sensitivity to NO x and

VOCs: results from the DISCOVER-AQ field experiment, Houston 2013. Atmospheric Chem. Phys. 16, 14463.

McClure, C.D., Jaffe, D.A., 2018. US particulate matter air quality improves except in wildfire-prone areas. Proc. Natl. Acad. Sci. https://doi.org/10.1073/pnas.1804353115.

Miller, J.D., Safford, H., 2012. Trends in wildfire severity: 1984 to 2010 in the Sierra Nevada, Modoc Plateau, and southern Cascades, California, USA. Fire Ecol. 8, 41–57.

Moritz, M.A., Parisien, M.-A., Batllori, E., Krawchuk, M.A., Van Dorn, J., Ganz, D.J., Hayhoe, K., 2012. Climate change and disruptions to global fire activity. Ecosphere 3, 1–22. https://doi.org/10.1890/ES11-00345.1

NIFC, 2018. National Interagency Fire Center. URL: https://www.nifc.gov/fireInfo/fireInfo_statistics.html (accessed 1.5.18).

Palancar, G.G., Lefer, B., Hall, S., Shaw, W., Corr, C., Herndon, S., Slusser, J., Madronich, S., 2013. Effect of aerosols and NO2 concentration on ultraviolet actinic flux near Mexico City during MILAGRO: measurements and model calculations. Atmospheric Chem. Phys. 13, 1011.

Pechony, O., Shindell, D.T., 2010. Driving forces of global wildfires over the past millennium and the forthcoming century. Proc. Natl. Acad. Sci. 107, 19167–19170.

Pfister, G., Emmons, L., Hess, P., Honrath, R., Lamarque, J., Val Martin, M., Owen, R., Avery, M., Browell, E., Holloway, J., 2006. Ozone production from the 2004 North American boreal fires. J. Geophys. Res. Atmospheres 111.

Real, E., Law, K.S., Weinzierl, B., Fiebig, M., Petzold, A., Wild, O., Methven, J., Arnold, S., Stohl, A., Huntrieser, H., 2007. Processes influencing ozone levels in Alaskan forest fire plumes during long-range transport over the North Atlantic. J. Geophys. Res. Atmospheres 112.

Reid, J., Koppmann, R., Eck, T., Eleuterio, D., 2005. A review of biomass burning emissions part II: intensive physical properties of biomass burning particles. Atmospheric Chem. Phys. 5, 799–825.

Roberts, J.M., 2007. PAN and Related Compounds, in: Volatile Organic Compounds in the Atmosphere. R. Koppmann (Ed.), doi:10.1002/9780470988657.ch6.

Rolph, G.D., Draxler, R.R., Stein, A.F., Taylor, A., Ruminski, M.G., Kondragunta, S., Zeng, J., Huang, H.-C., Manikin, G., McQueen, J.T., Davidson, P.M., 2009. Description and Verification of the NOAA Smoke Forecasting System: The 2007 Fire Season. Weather Forecast. 24, 361–378. https://doi.org/10.1175/2008WAF2222165.1.

Singh, H.B., Cai, C., Kaduwela, A., Weinheimer, A., Wisthaler, A., 2012. Interactions of fire emissions and urban pollution over California: Ozone formation and air quality simulations. Atmos. Environ. 56, 45–51. https://doi.org/10.1016/j.atmosenv.2012.03.046

Spracklen, D.V., Logan, J.A., Mickley, L.J., Park, R.J., Yevich, R., Westerling, A.L., Jaffe, D.A., 2007. Wildfires drive interannual variability of organic carbon aerosol in the western U.S. in summer. Geophys. Res. Lett. 34. https://doi.org/10.1029/2007GL030037

Spracklen, D.V., Mickley, L.J., Logan, J.A., Hudman, R.C., Yevich, R., Flannigan, M.D., Westerling, A.L., 2009. Impacts of climate change from 2000 to 2050 on wildfire activity and carbonaceous aerosol concentrations in the western United States. J. Geophys. Res. Atmospheres 114. https://doi.org/10.1029/2008JD010966

Urbanski, S., Hao, W., Nordgren, B., 2011. The wildland fire emission inventory: western United States emission estimates and an evaluation of uncertainty. Atmospheric Chem. Phys. 11, 12973–13000.

Val Martin, M., Heald, C.L., Lamarque, J.-F., Tilmes, S., Emmons, L.K., Schichtel, B.A., 2015. How emissions, climate, and land use change will impact mid-century air quality over the United States: a focus on effects at national parks. Atmos Chem Phys 15, 2805–2823. https://doi.org/10.5194/acp-15-2805-2015

Val Martin, M., Honrath, R., Owen, R.C., Pfister, G., Fialho, P., Barata, F., 2006. Significant enhancements of nitrogen oxides, black carbon, and ozone in the North Atlantic lower free troposphere resulting from North American boreal wildfires. J. Geophys. Res. Atmospheres 111.

Verma, S., Worden, J., Pierce, B., Jones, D., Al-Saadi, J., Boersma, F., Bowman, K., Eldering, A., Fisher, B., Jourdain, L., 2009. Ozone production in boreal fire smoke plumes using observations from the Tropospheric Emission Spectrometer and the Ozone Monitoring Instrument. J. Geophys. Res. Atmospheres 114.

Wang, T., Poon, C.., Kwok, Y.., Li, Y.., 2003. Characterizing the temporal variability and emission patterns of pollution plumes in the Pearl River Delta of China. Atmos. Environ. 37, 3539–3550. https://doi.org/10.1016/S1352-2310(03)00363-7

Westerling, A.L., 2016. Increasing western US forest wildfire activity: sensitivity to changes in the timing of spring. Philos. Trans. R. Soc. B Biol. Sci. 371. https://doi.org/10.1098/rstb.2015.0178

Westerling, A.L., Hidalgo, H.G., Cayan, D.R., Swetnam, T.W., 2006. Warming and Earlier Spring Increase Western U.S. Forest Wildfire Activity. Science 313, 940–943. https://doi.org/10.1126/science.1128834

Wigder, N.L., Jaffe, D.A., Saketa, F.A., 2013. Ozone and particulate matter enhancements from regional wildfires observed at Mount Bachelor during 2004–2011. Atmos. Environ. 75, 24–31. https://doi.org/10.1016/j.atmosenv.2013.04.026

Wood, S., 2018. Mixed GAM Computation Vehicle with Automatic Smoothness Estimation.

Wood, S.N., 2017. Generalized additive models: an introduction with R. CRC press.

Yokelson, R.J., Andreae, M.O., Akagi, S., 2013. Pitfalls with the use of enhancement ratios or normalized excess mixing ratios measured in plumes to characterize pollution sources and aging. Atmospheric Meas. Tech. 6, 2155.

Zhang, G., Mu, Y., Zhou, L., Zhang, C., Zhang, Y., Liu, J., Fang, S., Yao, B., 2015. Summertime distributions of peroxyacetyl nitrate (PAN) and peroxypropionyl nitrate (PPN) in Beijing: Understanding the sources and major sink of PAN. Atmos. Environ. 103, 289–296.

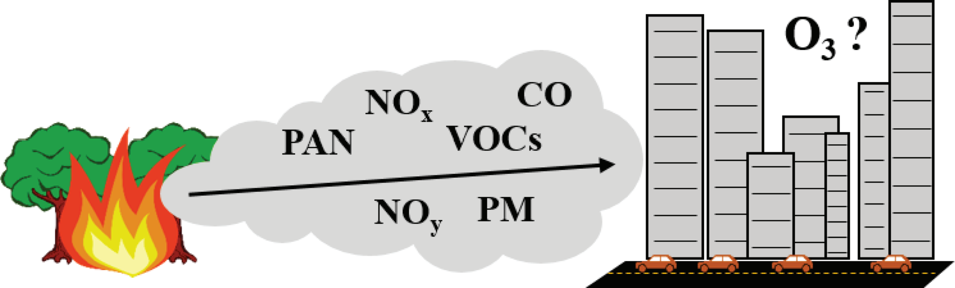

O_3 ?
NO_x
CO
PAN
VOCs
NO_y
PM